Tribol Lett (2008) 29:235–239
DOI 10.1007/s11249-008-9301-x

ORIGINAL PAPER

Robust Nanoadhesion Under Torque

S. H. Chen · G. Xu · A. K. Soh

Received: 13 September 2007 / Accepted: 24 January 2008 / Published online: 7 February 2008

Abstract In this article, optimization of shear adhesion strength between an elastic cylindrical fiber and a rigid substrate under torque is studied. We find that when the radius of the fiber is less than a critical value, the bonding–breaking along the contact interface occurs uniformly, rather than by mode III crack propagation. Comparison between adhesion models under torque and tension shows that nanometer scale of fibers may have evolved to achieve optimization of not only the normal adhesive strength but also the shear adhesive strength in tolerance of possible contact flaws.

Keywords Contact mechanics · Nanoadhesion · Shear strength · Torque

1 Introduction

In recent years, not only electronic devices but also mechanical devices have shown a trend toward miniaturization. Optimum design of such devices requires knowledge of mechanical and tribological properties of small structures. It is well known that the properties for micro- and nano-sized structures may differ significantly from those for macroscopic structures. Similarly, fracture features under different scales may show extreme changes between micro- and macroscopes. The theoretical strength of a solid is defined as the stress required to simultaneously break all the bonds across a fracture plane. In practice, the load-carrying capacity of a material has not been used most efficiently, and the apparent strength is reduced in contrast to the theoretical value due to crack-like flaws. Materials will fail via crack propagation due to the stress concentration near the crack tip. Since large flaws cannot occur in micro- or nanoscale structures, brittle fracture is less likely to occur in small structures, and the apparent strength should in general be much higher than that for macroscopic bodies [1].

In the adhesion problem, adhesive stress is determined by surface-to-surface separation. At a specific surface separation, the adhesive stress reaches its maximum value corresponding to the theoretical strength of adhesion. Generally speaking, the actual adhesion strength, which is defined as the force per unit contact area at pull-off, can be much lower than the theoretical adhesion strength due to the presence of crack-like flaws induced by surface roughness or contaminants. Under external loading, these adhesion flaws induce stress concentration near the contact edges and eventually lead to breakage of adhesion through crack propagation. In all these cases, the reduction of the apparent adhesion strength is caused by crack propagation. Conception of flaw tolerance or flaw insensitivity had been proposed recently, which means the adhesion strength can be maximized at the theoretical adhesion strength via size reduction [1–3]. The adhesive contact interface fracture is not due to the crack-like flaw propagation, but to a uniform bonding rupture. For example, Gao et al. [2] studied the adhesion strength of a flat-ended cylindrical punch in partial contact with a rigid substrate saturate and found that the adhesive strength will attain the theoretical strength below a critical scale. Persson [1] investigated the adhesive

S. H. Chen (✉) · G. Xu
LNM, Institute of Mechanics, Chinese Academy of Sciences, Beijing 100080, China
e-mail: shchen@lnm.imech.ac.cn

A. K. Soh
Department of Mechanical Engineering, The University of Hong Kong, Hong Kong, China
e-mail: aksoh@hkucc.hku.hk

problem of a rigid disk on an elastic half space and showed the strength saturation for small contacting objects. The minimum size of the adhesive systems guarantees robust adhesion. Hui et al. [4] and Glassmaker et al. [5] studied a bio-mimetic fibrillar structure with slender elastic fibrils distributed periodically and demonstrated that the adhesion strength can be enhanced in contrast to a non-fibrillar structure. Chen and Soh [6] found that the adhesion strength can be optimized by tuning the geometric parameters of a fibrillar structure. Northen and Turner [7] and Yao and Gao [8] reported significantly improved adhesion in hierarchical hairy adhesive materials. Structural hierarchy seems to play a critical role in robust adhesion.

In this article, we will study the torsion strength of a cylindrical fiber in adhesive contact with a rigid substrate. The main focus is on the relation of the shear-off strength and the scale of fibers.

It is found that there exists a critical size below which the shear tractions on the contact area will attain the theoretical shear strength uniformly. Most interestingly, the critical size under torque is quite consistent with that under tension for the nanometer structure, which means that nanometer fibers may have evolved to achieve optimization of not only the normal adhesive strength but also the shear adhesive strength in tolerance of possible contact flaws.

2 Flaw Tolerance Under Torque

A cylindrical fiber of radius R subjected to an external torque T and a very small tension force P in contact with a rigid substrate is discussed. Imperfect contact between the fiber and substrate is assumed as shown in Fig. 1, such that the radius of the actual contact area is $a = \lambda R$, $0 < \lambda < 1$. The outer rim $\lambda R < r < R$ represents flaws or regions of poor adhesion. The adhesive strength of such an adhesive joint can be calculated by treating the contact problem as a circumferentially cracked cylinder subjected to an external torque T and a small tension force P. The stress field near the edge of the contact area under torque T has a square root singularity with a mode III stress-intensity factor [9]

$$K_{\mathrm{III}} = \frac{2T}{\pi a^3}\sqrt{\pi a}F(\lambda) \quad \lambda = a/R \tag{1}$$

where $F(\lambda)$ can be expressed as

$$F(\lambda) = G(\lambda)\sqrt{1-\lambda} \tag{2}$$

and $G(\lambda)$ has relations with λ as follows,

$$G(\lambda) = \frac{3}{8}\left[1 + \frac{1}{2}\lambda + \frac{3}{8}\lambda^2 + \frac{5}{16}\lambda^3 + \frac{35}{128}\lambda^4 + 0.208\lambda^5\right] \tag{3}$$

Figure 2 shows the relation between λ and $F(\lambda)$, from which one can see that $F(\lambda)$ will decrease with an increasing value of λ. Some typical results of function $F(\lambda)$ with different values of λ are given in Table 1. $\lambda = 1$ corresponds to perfect contact or defect-free contact, in which case one can see that $F(\lambda)$ tends to be zero and the singularity vanishes.

Due to the very small force P that acted on the cylinder, the mode I component of the stress-intensity factor can be expressed as,

$$K_{\mathrm{I}} = \frac{P}{\pi a^2}\sqrt{\pi a}F_1(\lambda) \tag{4}$$

where $F_1(\lambda)$ varies in a narrow range between 0.4 and 0.5 for $0 \le \lambda \le 0.8$ and can be found in Gao et al. [2].

Substituting the stress-intensity factors Eqs. 1 and 4 into the Griffith energy balance criterion

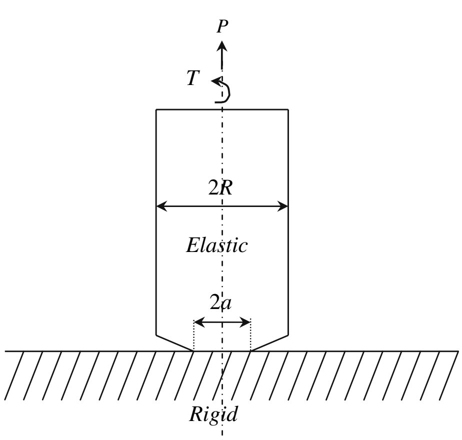

Fig. 1 Adhesion model of an elastic cylindrical fiber to a rigid substrate under an external torque T and a small tension force P. The contact area has a radius a, where $a < R$ and R is the radius of the fiber

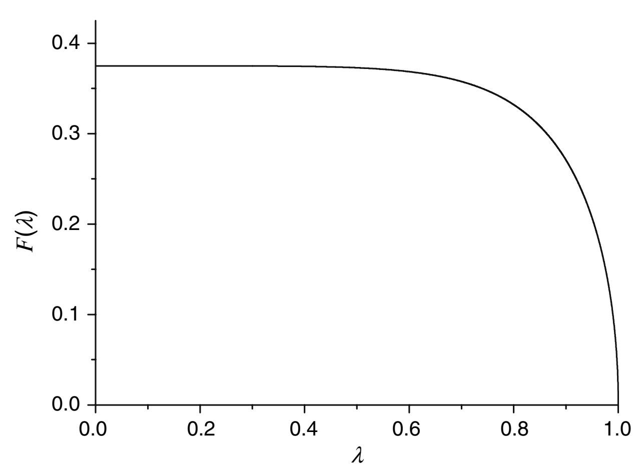

Fig. 2 The relation between the parameter λ ($\lambda = a/R$) and the function $F(\lambda)$ according to Eqs. 2 and 3

Table 1 Typical values of $F(\lambda)$ for different values of λ

λ	0	0.5	0.6	0.7	0.8	0.9
$F(\lambda)$	0.375	0.373	0.368	0.357	0.332	0.271

$$\frac{K_{\mathrm{I}}^2}{2E^*}+\frac{K_{\mathrm{III}}^2}{4\mu^*}=\Delta\gamma \tag{5}$$

yields

$$\frac{P^2F_1^2}{2E^*\pi a^3}+\frac{T^2F^2}{\mu^*\pi a^5}=\Delta\gamma \tag{6}$$

where factors 2 and 4 in Eq. 5 are due to the rigid substrate. $\mu^* = [1/\mu_1]^{-1}$ is the compound shear modulus with $\mu_1 = E_1/[2(1 + \nu_1)]$ for the cylindrical fiber and $\mu_2 \to \infty$ for the rigid substrate. $E^* = [(1-\nu_1^2)/E_1 + (1-\nu_2^2)/E_2]^{-1} = [(1-\nu_1^2)/E_1]^{-1}$ is the compound Young's modulus due to $E_2 \to \infty$. Equation 6 can be discussed according to three cases: (1) approximately pure tension case when the torque is very small and the energy produced by torque can be neglected in contrast to that produced by tension, (2) approximately pure shear case when the tension force is very small, (3) the energies contributed by tension force and torque are comparable. The first case has been investigated by Gao et al. [2] and the third case will be investigated later. We investigate only the second case in the present article.

For the case with a very small tension force P, the first term in Eq. 6 can be omitted, so that the torque can be obtained as

$$T=\frac{a^2}{F}\sqrt{\pi\mu^*\Delta\gamma a} \tag{7}$$

where $\Delta\gamma=\gamma_1+\gamma_2-2\gamma_{12}$ denotes the work of adhesion of the contact interface or the change in the interfacial energy per unit area; γ_1, γ_2 are the intrinsic surface energies of the two solids; and γ_{12} is the surface energy of the contact interface.

Also we know that all the stress components on the contact interface under torque vanish except the stress component $\tau_{z\theta}$ (cylindrical coordinate system r,θ,z is assumed to attach at the center of the contact area). The equilibrium condition leads to

$$T=2\pi\int_0^a \tau_{z\theta}r^2\mathrm{d}r \tag{8}$$

Generally, the stress component $\tau_{z\theta}$ is a function of radius r of the contact area and has a square root singularity at the contact edge $r = a$. Also we know that uniform shear traction can be obtained for an interface between an elastic solid and a rigid one. Thus, we assume that the bond breaking occurs uniformly over the contact area under torque, and the shear-off stress is then independent of the radius a of the contact area, i.e.,

$$\tau_{z\theta}=\tau_{\mathrm{th}} \tag{9}$$

Substituting Eq. 9 into Eq. 8 yields the shear-off torque,

$$T_c=\frac{2\pi a^3}{3}\tau_{\mathrm{th}} \tag{10}$$

The apparent adhesive shear strength normalized by the theoretical strength is obtained as

$$\begin{aligned}\hat{\tau}_c&=\frac{T}{(2\pi R^3\tau_{\mathrm{th}}/3)}=\frac{3}{2F\sqrt{\pi}}\lambda^{5/2}\sqrt{\frac{\mu^*\Delta\gamma}{\tau_{\mathrm{th}}^2R}}\\&=\frac{3}{2F\sqrt{\pi}}\lambda^{5/2}\psi\end{aligned} \tag{11}$$

where

$$\psi=\sqrt{\frac{\mu^*\Delta\gamma}{\tau_{\mathrm{th}}^2R}} \tag{12}$$

The maximum adhesive shear strength is achieved when the shear-off torque reaches $T_c=\frac{2\pi a^3}{3}\tau_{\mathrm{th}}$, then

$$\hat{\tau}_{c\,\max}=\lambda^3 \tag{13}$$

in which the traction within the contact area uniformly reaches the interface theoretical strength τ_{th}. This saturation in strength occurs when the following identity is satisfied,

$$\frac{3}{2F\sqrt{\pi}}\lambda^{-1/2}\psi=1 \tag{14}$$

which yields a critical radius of the fiber R_{cr}; when the radius R of the fiber is not larger than R_{cr} (i. e., $R \le R_{\mathrm{cr}}$) bond breaking may occur uniformly over the contact area and the stress concentration near the edge of the contact area vanishes. The shear-off stress attains the theoretical stress τ_{th} and the shear-off torque is $2\pi a^3\tau_{\mathrm{th}}/3$. The critical radius of the fiber can be written as

$$R_{\mathrm{cr}}=\frac{9\mu^*\Delta\gamma}{4\pi\lambda F^2\tau_{\mathrm{th}}^2} \tag{15}$$

The apparent adhesive strength via the non-dimensional parameter ψ for different values of λ is plotted in Fig. 3.

3 Comparison Between Tension and Torque Cases

In practice, interfacial crack-like flaws due to surface roughness or contaminants inevitably weaken the actual adhesion strength. Gao et al. [2] performed finite element calculations to show the adhesion strength of a flat-ended cylindrical punch in partial contact with a rigid substrate saturate at the theoretical strength below a critical radius around 200 nm for the normal interaction. What is the effect of nanometer length scale for adhesion under torque?

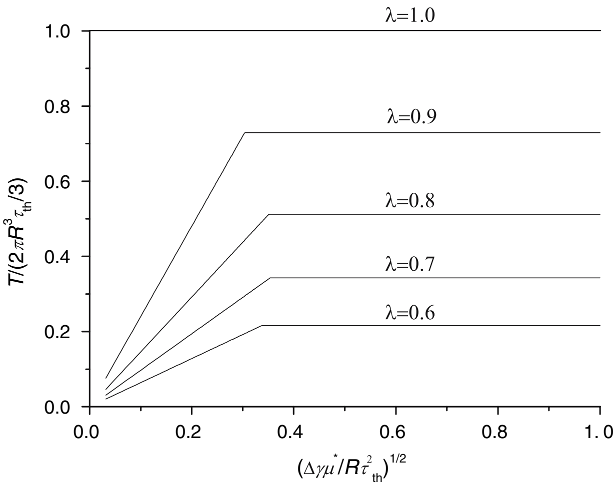

Fig. 3 Plots of the apparent shear adhesion strength for different actual contact areas (denoted by λ) according to the Griffith criterion and the theoretical shear strength

Similar to [2], an elastic cylindrical fiber adhering to a rigid substrate is modeled; then

$$\mu^* = \mu_1 = \frac{E_1}{2(1+v_1)} \tag{16}$$

According to [10] the frictional stress of nanoscale commensurate contacts should be constant and of the order of the theoretical shear strength of the material. This is in good agreement with experimental results [11–13], where the frictional stress $\tau_f \sim \mu/43$. In general, the value of τ_f measured in the AFM for nanoscale contacts may be considered as an effective theoretical shear strength of the interface, so that we take the theoretical shear strength of the contact interface as

$$\tau_{th} = \frac{1}{43}\mu_1 \tag{17}$$

The parameters for the contact interface are selected as the same as those in [2]:

$$\Delta\gamma = 0.01\,J/m^2 \quad E_1 = 2\,\mathrm{GPa} \quad v = 0.3 \tag{18}$$

From above the theoretical shear strength is

$$\tau_{th} \approx 17.89\,\mathrm{MPa} \tag{19}$$

Assume that the actual contact area is about 50% of the total area available for contact, which corresponds to $\lambda \approx 0.7$. The critical size for shear strength saturation is given as

$$R_{cr} = 192\,\mathrm{nm} \tag{20}$$

Comparing the critical size for shear strength saturation to that for normal strength saturation (about 225 nm in [2]), one can see that both are very close. The above analysis suggests that the nanometer size of fibers may have evolved to achieve optimization of not only the normal adhesive strength but also the shear adhesive strength in tolerance of possible contact flaws.

Table 2 Critical size R_{cr} for different contact areas (denoted by λ) with the parameters $\Delta\gamma = 0.01\,J/m^2, E_1 = 2\,\mathrm{GPa}, v = 0.3$

λ	0.5	0.6	0.7	0.8	0.9
R_{cr} (nm)	247	211	192	195	260

Table 2 gives the critical size for shear strength saturation for different contact areas. One can see that all the values lie in the range of 150–250 nm, which is quite consistent with the critical size under tension [2].

4 Summary

Nanoadhesion between an elastic cylindrical fiber and a rigid substrate has been analyzed considering that an external torque acted on the fiber. The critical size of the fiber has been found, below which the singularity of the shear stress on the contact interface vanishes, and it will attain uniformly the theoretical shear strength of the interface. The comparison between the torque and tension cases shows that the nanometer scale of fibers may have evolved to achieve maximum adhesion strength not only under tension but also under torque, which highlights the prevalence of flaw tolerance design in bio-mimetic engineering.

Acknowledgments The work reported here is supported by NSFC (10672165, 10732050, 10721202) and KJCX2-YW-M04.

References

1. Persson, B.N.J.: Nanoadhesion. Wear **254**, 832–834 (2003)
2. Gao, H., Wang, X., Yao, H., Gorb, S., Arzt, E.: Mechanics of hierarchical adhesion structures of geckos. Mech. Mater. **37**, 275–285 (2005)
3. Gao, H., Chen, S.: Flaw tolerance in a thin strip under tension. J. Appl. Mech. **72**, 732–737 (2005)
4. Hui, C.Y., Glassmaker, N.J., Tang, T., Jagota, A.: Design of biomimetic fibrillar interface: 2. Mechanics of enhanced adhesion. J. R. Soc. Interface **1**, 35–48 (2004)
5. Glassmaker, N.J., Jagota, A., Hui, C.Y., Kim, J.: Design of biomimetic fibrillar interface: 1. Making contact. J. R. Soc. Interface **1**, 23–33 (2004)
6. Chen, S.H., Soh, A.K.: Tuning the geometrical parameters of biomimetic fibrillar structures to enhance adhesion. J. R. Soc. Interface **5**, 373–382 (2008)
7. Northen, M.T., Turner, K.L.: A batch fabricated biomimetic dry adhesive. Nanotechnology **16**, 1159–1166 (2005)
8. Yao, H., Gao, H.: Mechanics of robust and releasable adhesion in biology: bottom-up designed hierarchical structures of gecko. J. Mech. Phys. Solids **54**, 1120–1146 (2006)
9. Tada, J., Paris, P.C., Irwin, G.R.: The Stress Analysis of Cracks Handbook. ASME Press, New York (2000)

10. Hurtado, J.A., Kim, K.S.: Scale effects in friction of single-asperity contacts. I. From concurrent slip to single-distribution-assisted slip. Proc. R. Soc. Lond. A **455**, 3363–3384 (1999)
11. Carpark, R.W., Agrait, N., Ogletree, D.F., Salmeron, M.: Measurement of the interfacial shear (friction) with an ultrahigh vacuum atomic force microscope. J. Vac. Sci. Technol. B **14**, 1289–1295 (1996)
12. Carpick, R.W., Agrait, N., Ogletree, D.F., Salmeron, M.: Variation of the interfacial shear strength and adhesion of a nanometer sized contact. Langmuir **12**, 3334–3340 (1996)
13. Lantz, M.A., O'Shea, S.J., Welland, M.E., Johnson, K.L.: Atomic-force-microscope study of contact area and friction on $NbSe_2$. Phys. Rev. B **55**, 10776–10785 (1997)